The β_{1a} subunit is essential for the assembly of dihydropyridine-receptor arrays in skeletal muscle

Johann Schredelseker*, Valentina Di Biase†, Gerald J. Obermair‡, E. Tatiana Felder*, Bernhard E. Flucher‡, Clara Franzini-Armstrong†§, and Manfred Grabner*§

Departments of *Medical Genetics, Molecular and Clinical Pharmacology and ‡Physiology and Medical Physics, Innsbruck Medical University, A-6020 Innsbruck, Austria; and †Department of Cell and Developmental Biology, University of Pennsylvania, Philadelphia, PA 19104

Contributed by Clara Franzini-Armstrong, October 5, 2005

Homozygous zebrafish of the mutant *relaxed* (*red*^{ts25}) are paralyzed and die within days after hatching. A significant reduction of intramembrane charge movements and the lack of depolarization-induced but not caffeine-induced Ca^{2+} transients suggested a defect in the skeletal muscle dihydropyridine receptor (DHPR). Sequencing of DHPR cDNAs indicated that the α_{1S} subunit is normal, whereas the β_{1a} subunit harbors a single point mutation resulting in a premature stop. Quantitative RT-PCR revealed that the mutated gene is transcribed, but Western blot analysis and immunocytochemistry demonstrated the complete loss of the β_{1a} protein in mutant muscle. Thus, the immotile zebrafish *relaxed* is a β_{1a}-null mutant. Interestingly, immunocytochemistry showed correct triad targeting of the α_{1S} subunit in the absence of β_{1a}. Freeze-fracture analysis of the DHPR clusters in *relaxed* myotubes revealed an ≈2-fold reduction in cluster size with a normal density of DHPR particles within the clusters. Most importantly, DHPR particles in the junctional membranes of the immotile zebrafish mutant *relaxed* entirely lacked the normal arrangement in arrays of tetrads. Thus, our data indicate that the lack of the β_{1a} subunit does not prevent triad targeting of the DHPR α_{1S} subunit but precludes the skeletal muscle-specific arrangement of DHPR particles opposite the ryanodine receptor (RyR1). This defect properly explains the complete deficiency of skeletal muscle excitation–contraction coupling in β_1-null model organisms.

calcium channels | excitation–contraction coupling | tetrads | zebrafish

Excitation–contraction (EC) coupling is understood as the signal transduction process connecting membrane depolarization to the contraction of muscle cells. This process is initiated by the concerted action of two Ca^{2+} channels, the plasmalemmal voltage-gated dihydropyridine receptor (DHPR) and the sarcoplasmic reticulum (SR) ryanodine receptor (RyR). In junctions of the SR with the plasma membrane (peripheral couplings) or with the transverse tubules (triads), membrane depolarization is sensed by the DHPR, which then triggers RyR opening and Ca^{2+} release from the SR. In skeletal muscle cells, this signal-transduction is independent of Ca^{2+} influx through the DHPR (1) but depends on protein–protein interaction between the DHPR and the RyR1 (2, 3). This physical coupling requires the coordinated arrangement of DHPRs and RyR1s in the junctions. In skeletal muscle triads and peripheral couplings, groups of four DHPRs (tetrads) are arranged in orthogonal arrays matching the opposing RyR1 arrays (4). Formation of DHPR tetrads requires the presence of RyR1.

The skeletal muscle DHPR complex is composed of the voltage-sensing and pore-forming α_{1S} subunit and the auxiliary subunits β_{1a}, $\alpha_2\delta$-1, and γ (5). Targeted deletions of the $\alpha_2\delta$-1 and γ subunits do not critically interfere with EC coupling function (6, 7). In contrast, α_{1S} and β_{1a} subunit null-mutant mice display a lack of EC coupling and, thus, lethal muscle paralysis (8, 9). Although failure of EC coupling is obvious in the α_{1S}-null (dysgenic) mouse muscle, which lacks the voltage-sensor, the molecular mechanism leading to the complete lack of EC coupling in the β_{1a}-null mice is not fully understood (8). Myotubes from β_{1a}-null mice show reduced L-type Ca^{2+} currents, charge movements, and 1,4-dihydropyridine binding (10). The staining intensity for α_{1S} in immunocytochemistry was initially described to be below detectability (8), but later it was found to be significantly higher than that of dysgenic myotubes (11). Therefore, it remained unclear whether the loss of EC coupling in β_{1a}-null myotubes was caused by decreased membrane expression of DHPRs, or by the lack of a specific contribution of the β subunit to the EC coupling mechanism (10, 12).

We addressed this question in the paralyzed zebrafish mutant *relaxed* (13), for which a defect in the EC coupling apparatus had been proposed (14). Using molecular biology, protein biochemistry, and immunocytochemistry techniques, we show that the zebrafish mutant *relaxed* lacks the DHPR β_{1a} subunit. In contrast to previous studies (8, 11), we can use this novel model organism to demonstrate that the α_{1S} is correctly targeted into skeletal muscle triad junctions in the absence of β_{1a}. However, DHPRs lacked the skeletal muscle-specific arrangement in tetrads and displayed substantially reduced charge movement. Therefore, a disruption of functional DHPR-RyR interactions caused by the lack of the β_{1a} subunit is responsible for the paralysis of skeletal muscle in β_1-null muscle cells.

Materials and Methods

Zebrafish Strain. Zebrafish of the strain *red*^{ts25} (*relaxed*) (13) were obtained from the Max Planck Institute in Tübingen, Germany. After cross breeding of heterozygous parents, homozygous *relaxed* larvae were identified by the inability to move in response to tactile stimuli. Larvae with a normal phenotype (heterozygous and wild type) were used for control experiments and will be collectively referred to as "normal."

Isolation of Myocytes. Larvae were anesthetized with MS-222 (Sigma) and decapitated, and the tails were digested for 1 h in 200 units/ml collagenase in Hanks' solution (Sigma) with continuous trituration. Myotubes were plated on collagen-coated plastic dishes or glass cover slips and cultured in 60% L-15 medium (Sigma) with 3% FCS and 3% horse serum (Invitrogen) at 28°C for 12–72 h.

Biophysical Characterization. For field stimulation experiments, myotubes from 3- to 4-day-old larvae were incubated with 5 μM Fluo-4 AM plus 0.01% Pluronic F-127 (Molecular Probes) in 60% L-15 medium. Action potentials were elicited by applying extracellular electrical stimuli (0.5 Hz, 25 V/cm electrode distance, 1 ms). Ca^{2+} signals (Fluo-4) were recorded by a photo-

PHYSIOLOGY

Conflict of interest statement: No conflicts declared.

Abbreviations: EC, excitation–contraction; DHPR, dihydropyridine receptor; SR, sarcoplasmic reticulum; RyR, ryanodine receptor; WGS, whole genome shotgun.

Data deposition: The sequences reported in this paper have been deposited in the GenBank database (accession nos. AY952462 and AY495698).

§To whom correspondence may be addressed. E-mail: manfred.grabner@uibk.ac.at or armstroc@mail.med.upenn.edu.

meter system (PTI, South Brunswick, NJ) mounted on a Zeiss Axiovert epifluorescence microscope (15).

Whole-cell patch clamp recordings of Ca^{2+} currents, intracellular Ca^{2+} transients, and intramembrane charge movements were performed as recently described for mouse myotubes (16, 17). The following modifications were applied to eliminate a robust Ca^{2+}-activated Cl^- current in zebrafish muscle cells[¶]: The bath solution contained 10 mM $Ca(OH)_2$, 100 mM L-aspartate, and 10 mM Hepes (pH 7.4 with tetraethylammonium hydroxide). Contractions of myotubes were blocked by adding 100 μM *N*-benzyl-*p*-toluene sulfonamide (Sigma) (18). Patch pipettes had resistances of 3–5 MΩ when filled with 145 mM CsAspartate, 10 mM Hepes, 0.5 mM CsEGTA, and 3 mM MgATP (pH 7.4 with CsOH).

Sequence Analysis. α_{1S} and β DHPR subunit cDNAs and genomic DNAs from wild type zebrafish and from homozygous *relaxed* larvae were PCR amplified by using the *Pfu Turbo* DNA polymerase (Stratagene) and sequenced (MWG Biotech). Total RNA was isolated by using the RNeasy Mini kit (Qiagen) and reverse transcribed by using the Ready-To-Go T-primed first-strand kit (Amersham Pharmacia). Genomic DNA was isolated according to the QIAamp DNA Mini kit protocol (Qiagen).

α_{1S} cDNA. 12 overlapping fragments (≈650 bp) were obtained by RT-PCR. Primers were designed according to zebrafish whole genome shotgun (WGS)-trace exon sequences identified by a NCBI BLAST search with carp α_{1S} cDNA (19) as template. The sequenced zebrafish α_{1S} was deposited in the GenBank database (accession no. AY495698).

β_{1a} cDNA. A zebrafish β_{1a}-specific PCR primer pair was designed according to the outermost 5′ and 3′ exon sequences that could be identified by a NCBI zebrafish WGS-trace BLAST search using rabbit β_{1a} (20) as template. The zebrafish β_{1a} RT-PCR fragment (nucleotides 96–1493; GenBank accession no. AY952462) was derived from adult wild-type cDNA. For sequence analysis, a blunt-HindIII fragment (nucleotides 96–1353) was cloned into the SmaI/HindIII polylinker site of pBluescript SK+ (Stratagene). The derived sequence was used to identify exons 2–13 of β_{1a} by a WGS-trace BLAST search. Exon 1 was identified using the Universal GenomeWalker kit (Clontech). Exon-flanking intron primer pairs were designed to sequence all 13 exons and exon–intron transitions from wild-type and mutant *relaxed*.

Quantitative TaqMan PCR. Normal and *relaxed* cDNA was generated as described above. The relative abundance of β_1 subunit mRNA was assessed by TaqMan quantitative PCR (50 cycles) using the comparative C_T method (Applied Biosystems) and the β-actin transcript as reference. Total RNA (7.6 ng) equivalents of cDNA and the specific TaqMan Gene Expression Assay were used for each 20-μl reaction in TaqMan Universal PCR Master Mix (Applied Biosystems). RNA samples without reverse transcriptase and samples without template were routine controls. Analysis was performed by using the Mx4000 Multiplex Quantitative PCR System (Stratagene). Custom TaqMan Gene Expression Assays were designed to span exon–exon boundaries: Exons 2/3 of zebrafish β_{1a} mRNA and exons 3/4 of zebrafish β-actin mRNA (GenBank accession no. NM131031). Exon–intron structures of β-actin and Ca^{2+} channel β_{1a} subunit genes were derived from NCBI BLAST searches of the zebrafish WGS trace database.

Immunostaining. Myotubes from 3- to 4-day-old larvae were cultured for 1 day on glass cover slips, fixed with either 100% methanol (10 min at −20°C) or 4% paraformaldehyde in 0.1 M phosphate buffer (20 min at room temperature) and immunostained as described (15). Antibodies were mAb 1A against α_{1S} (Affinity Bioreagents, ref. 21) at 1:2,000–30,000 (see below), mAb 20A against $\alpha_2\delta$-1 (22) at 1:1,000, sequence-directed pan-β antibody RCP6 (23) at 1:2,000, and mAB 34-C against RyR (Alexis Biochemicals, Lausen, Switzerland) at 1:2,000 Alexa-conjugated goat-anti-rabbit and goat-anti-mouse (Molecular Probes) were used as secondary antibodies. Omission of primary antibodies was routinely performed as controls. Experiments were repeated at least three times.

For quantification of α_{1S} expression in normal and *relaxed* myotubes mAB 1A dilutions of 1:2,000, 1:10,000, 1:20,000, and 1:30,000 were used to confirm the linearity and reproducibility of the fluorescence signal. Cultures were immunostained simultaneously, and images were acquired with identical exposure times after background subtraction and shading correction. Average fluorescence intensity was recorded along a line across a row of α_{1S} clusters (triadic junctions) in five measurements on each myotube, with 10 myotubes analyzed for each condition and antibody dilution in each of three different cultures. Statistical significance was determined by paired Student's *t* test (group: cell preparation/AB dilution).

Western Blot. For total membrane protein preparation ≈300 tails of *relaxed* and normal larvae (4–6 days old), as well as skeletal muscle tissue from an adult zebrafish were ultrasonicated in 10 mM Tris·HCl with 10 mM EDTA and 5 μl/ml Proteinase Inhibitor Mixture for mammalian tissues (Sigma). After centrifugation at 400 × *g*, the supernatant was centrifuged at 50,000 × *g* to precipitate membrane fractions. Pellets were resuspended in the buffer described above. Rabbit muscle protein was isolated as described (24) and used as a control. Isolated protein (10 μg per lane) was loaded for β_{1a} blots, and 15–50 μg was loaded for α_{1S} blots and separated by SDS/PAGE (NuPage 4–12% Bis-Tris gel with NuPage Mops SDS running buffer, both Invitrogen) at 200 V for 60 min.

Proteins were blotted to an Immobilon-P polyvinylidene difluoride membrane (Millipore) using Tris-Glycine buffer with NuPAGE antioxidant (Invitrogen). For blotting of the β subunit protein (1.5 h at 200 mA), 10% methanol was added to the buffer; for the hydrophobic, high molecular weight α_{1S} subunit (1 h at 100 V), 20% methanol and 0.1% SDS was added. After blocking (4% dry milk for 1 h), membranes were incubated overnight with primary antibodies RCP6 or mAB 1A, respectively, and detected with the HRP-system (ECL, Amersham Pharmacia).

Freeze Fracture Electron Microscopy. Myoblasts from 1-day-old larvae were cultured on Thermanox (Nalge Nunc) for 3 days until fusion, rinsed in PBS, and fixed with 6% glutaraldehyde in 0.1 M cacodylate buffer (both Sigma) at neutral pH at ≈23°C. Samples were stored in 2% glutaraldehyde at 4°C until processing for freeze-fracture. All other procedures and solutions have been recently described for fracturing mouse myotubes (25). For thin sectioning and freeze-fracture, 26- to 72-h-old larvae were fixed in 6% glutaraldehyde after removing the tail skin and processed as in ref. 4.

Statistics. Statistical significance from experimental approaches was determined by unpaired Student's *t* test, and data are reported as mean ± SEM, unless noted otherwise.

Results and Discussion

Phenotype and Genotype of the Zebrafish Mutant *relaxed*. The zebrafish mutant *relaxed* was obtained from a large-scale mutagenesis screen (26) and is characterized by complete skeletal muscle paralysis (13). Previous work indicated a defect in the EC

[¶]Schredelseker, J., Flucher, B. E., Kugler, G. & Grabner, M. (2004) *Biophys. J.* **86**, 63a (abstr.).

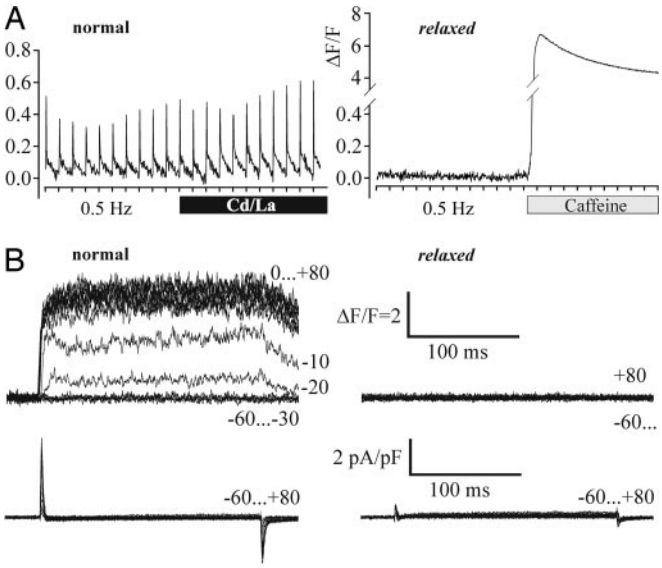

Fig. 1. Myotubes from zebrafish mutant *relaxed* lack EC coupling. (*A*) Recordings of action-potential-induced intracellular Ca^{2+} transients from dissociated myotubes of larval tail muscle loaded with the fluorescent Ca^{2+} indicator Fluo-4 AM. Tick marks on the *x* axes indicate electrical stimuli in 2-s intervals. Normal myotubes (*Left*) responded to 1-ms stimuli with Ca^{2+} transients that persisted after applying 0.5 mM Cd^{2+} and 0.1 mM La^{3+} (black bar). Myotubes isolated from zebrafish *relaxed* failed to display action-potential-induced Ca^{2+} transients (*Right*), even though Ca^{2+} release could be evoked with 6 mM caffeine (shaded bar), indicating intact loading of SR stores and functional RyR (n = 5 and 4, respectively). (*B*) Simultaneous recordings of depolarization-induced Ca^{2+} transients (*Upper*) and whole-cell Ca^{2+} currents (*Lower*) from normal (*Left*) and *relaxed* (*Right*) myotubes. Step depolarizations (200-ms pulses) to membrane potentials between −60 and +80 mV were applied in 10-mV increments from a holding potential of −80 mV following a prepulse protocol (17). Changes in the cytoplasmic free [Ca^{2+}] were measured with Fluo-4 and are displayed as $\Delta F/F$. Note that, in both normal and *relaxed* myotubes, I_{Ca} was never detected ($n > 30$).

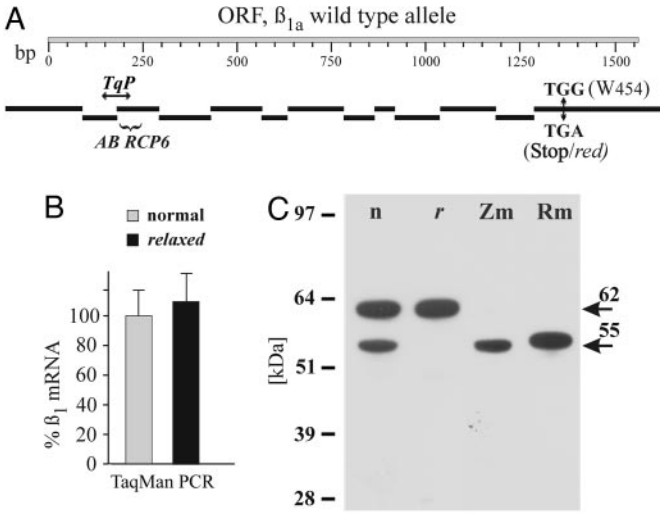

Fig. 2. The DHPR β_{1a} subunit of zebrafish *relaxed* is transcribed as mRNA but not expressed as protein. (*A*) Schematic representation of the 13 β_{1a} exons (black bars) aligned to the ORF (ORF, shaded bar) of its cDNA (GenBank accession no. AY952462). Numbers designate base pairs. TGG (W454) ↔ TGA (Stop/*red*) indicates the position of the point mutation in exon 13 leading to a premature stop in β_{1a} of *relaxed*. TqP shows the position of the TaqMan probe. The parentheses indicate the epitope of pan-β antibody RCP6. (*B*) β_1 mRNA transcription in *relaxed* normalized to normal zebrafish assessed by TaqMan quantitative PCR. Mean values of two individual experiments, from each of two separate cDNA preparations, are shown and are statistically indistinguishable (P = 0.87). Statistical significance was determined by using the ΔC_T values in a paired student's t test (group, RNA preparation/TaqMan assay). (*C*) Western blot analysis (one representative experiment of nine is shown) with pan-β antibody RCP6 indicated that a 55-kDa β band (lower arrow) is expressed in normal larval tail (n) and adult zebrafish muscle (Zm) but is lacking in *relaxed* tail preparations (*r*). The 62-kDa protein band (upper arrow) in both larval tail preparations most probably represents another β isoform originating from other larval tissues (e.g., spinal cord). Pure skeletal muscle preparations from adult normal zebrafish (Zm) and from rabbit (Rm) do not contain this 62-kDa isoform.

coupling complex, most likely in the DHPR (14). To identify the molecular mechanism underlying the EC coupling defect, we first analyzed the response of myotubes from normal and *relaxed* zebrafish larvae to electrical field stimulation. As expected for skeletal muscle EC coupling, normal myotubes showed pronounced action-potential-induced intracellular Ca^{2+} transients, which were insensitive to L-type Ca^{2+} channel block by Cd^{2+} and La^{3+} (Fig. 1*A*). *Relaxed* myotubes did not respond to electrical stimulation, although the subsequent addition of 6 mM caffeine caused a strong Ca^{2+} transient, indicating that RyR-dependent SR Ca^{2+} release was fully functional. To exclude the possibility of a defect in muscle membrane excitability, whole-cell patch clamp analysis of L-type Ca^{2+} currents, combined with fluorometric recordings of depolarization-induced intracellular Ca^{2+} release, was performed (Fig. 1*B*). In normal myotubes, depolarizations to potentials between −20 and +80 mV induced robust Ca^{2+} transients with a mean $\Delta F/F_{max}$ of 4.6 ± 0.6 (n = 9). However, depolarization-induced Ca^{2+} transients were never observed in *relaxed* myotubes (n = 6). Thus, the defect in EC coupling is located downstream of depolarization and upstream of SR Ca^{2+} release, pointing to a failure of voltage-sensing or the allosteric transmission of this signal to the RyR1.

To our surprise L-type Ca^{2+} currents were absent in both normal and *relaxed* myotubes (Fig. 1*B Lower*). Thus, the zebrafish DHPR is a non-Ca^{2+}-conducting voltage sensor, and this organism provides *in vivo* evidence that skeletal muscle EC coupling is fully functional without Ca^{2+} influx through the DHPR.

Because the functional evidence suggested a defective DHPR in *relaxed* muscle and because only two of the four DHPR subunits (α_{1S} and β_{1a}) cause paralysis in null-mutant mice, we searched for a mutation in these subunits. Sequencing of α_{1S} cDNA revealed no sequence deviations between wild-type and *relaxed* zebrafish. However, cloning and sequencing of the β_{1a} cDNA and, consequently, of all 13 β_{1a} exons and exon–intron transitions from wild-type and *relaxed* zebrafish identified a point mutation ($G_{1362}A$) in exon 13 (Fig. 2*A*). The ORF of the wild-type β_{1a} subunit mRNA encodes for a 520-aa protein (M_r 57,445) with 76% sequence identity to rabbit β_{1a}, but only 52, 43, and 42% to the rabbit β_2, β_4, and β_3 subunits, respectively. The G–A point mutation in exon 13 of *relaxed* β_{1a} DNA leads to the premature termination at the position of Trp-454. The observed fraction of 24.6% (n = 896) paralyzed offspring when mating heterozygous adults is consistent with the monogenetic heredity of the EC coupling defect (27).

The Zebrafish *relaxed* Is a β_{1a}-Null Mutant. According to the recently published β subunit crystal structure (28, 29), the mutation would lead to a β_{1a} protein that is truncated within the most C-terminal α-helix of the guanylate kinase domain. Because the consequences of this premature stop were not predictable, we analyzed the expression of the mutated β_{1a} mRNA and protein. Using quantitative TaqMan PCR, we measured similar levels of β_1 transcripts in normal and *relaxed* larvae (Fig. 2*B*), excluding a decreased stability of the message. Western blot analysis of preparations from normal zebrafish larvae (Fig. 2*C*) using the pan-β antibody RCP6 (23) directed against an epitope near the

PHYSIOLOGY

N terminus (see Fig. 2*A*) revealed two specific bands at 55 and 62 kDa. Both bands could be completely blocked by antigen preincubation of the antibody (23). Most importantly, the 55-kDa band was absent in preparations from *relaxed* larvae (Fig. 2*C*). This band was identified as the skeletal muscle β_{1a} homolog of zebrafish based on the following evidence: It was the exclusive protein labeled in pure muscle preparations from normal adult zebrafish, its size agrees with the published molecular mass of rabbit β_{1a} (52–56 kDa) (23), as well as with the calculated M_r for zebrafish β_{1a} (57 kDa), and it is clearly apart from the 62- to 88-kDa range of β_{1b}–β_4 (23). The higher molecular mass band found in the tail preparations from larvae most likely represents a homologue of another β isoform expressed in neuronal or smooth muscle tissue present in this preparation. Technical limitations did not allow isolation of pure muscle tissue from the ≈5-mm small larvae, which were used before *relaxed* larvae die at day 6–7.

Next, expression of the DHPR β_{1a} subunit was analyzed with immunolabeling of myotubes isolated from normal and *relaxed* zebrafish (Fig. 3). Double immunofluorescence labeling with antibodies against the β subunit and RyR1 showed that, in normal myotubes, the DHPR β_{1a} subunit and the Ca^{2+} release channel are colocalized in transverse lines of clusters representing transverse tubule/SR junctions. Whereas the expression pattern of RyR1 is unaltered in myotubes of *relaxed* zebrafish, the specific β_{1a} signal was absent.

Together, the specific lack of the lower β band in the Western blot analysis and the specific lack of the immunofluorescence signal in the samples from *relaxed* zebrafish clearly demonstrate the absence of the β_{1a} protein in the mutant. Thus, the premature stop codon in the β_{1a} transcript results either in deficient translation or in the immediate posttranslational degradation of the truncated protein. Truncation of up to 60 C-terminal residues had no adverse effect on expression of β chimeras in β_1-null myotubes (30). In contrast, the data presented here show that the *relaxed* β_{1a} protein, which lacks 67 C-terminal residues, is totally lost. The difference might be due to the fact that the mutant zebrafish β_{1a} is truncated within the most C-terminal α-helical region of the guanylat kinase domain (28, 29), and thus affects a major structural element, which may be essential for proper expression. Alternatively, quality control mechanisms, which apply for endogenously expressed proteins, may have been bypassed in the heterologous expression experiments (30).

The Lack of β_{1a} in Zebrafish *relaxed* Does Not Impede α_{1S} Triad Targeting, but Results in a Failure of Skeletal Muscle-Specific Arrangement of DHPRs vis-à-vis the RyR1. The results presented so far demonstrated that the immotile zebrafish *relaxed* is a β_1-null mutant. So, how does the lack of the β_{1a} protein affect expression and function of the DHPR in skeletal muscle? Based on extensive coexpression experiments in heterologous systems (31, 32) and on results from the β_{1a}-null mouse (8, 11), a lack of α_{1S} triad expression would have been expected. However, immunofluorescence analysis of the fully differentiated zebrafish myotubes clearly demonstrated that β_{1a} deficient cells are able to correctly target α_{1S} into the triads (Fig. 3). This finding is in contrast to previous work describing α_{1S} as only weakly expressed and located in a diffuse, nonclustered distribution. Thus, in native muscle, β_{1a} is not essential for triad targeting of the DHPR. Nonetheless, quantification of the α_{1S} immunofluorescence showed that in myotubes of the *relaxed* mutant the intensity of the signal was only about half (44 ± 4%) of that in normal myotubes (Fig. 4*A*). The reduction in α_{1S} immunolabeling is consistent with a similar reduction of α_{1S} protein measured in Western blots (45 ± 6%; Fig. 4*B*).

Previously, we demonstrated that, in the absence of the α_{1S} subunit, $\alpha_2\delta$-1 is expressed but mistargeted into the plasma membrane (7, 33). Accordingly, in normal zebrafish myotubes,

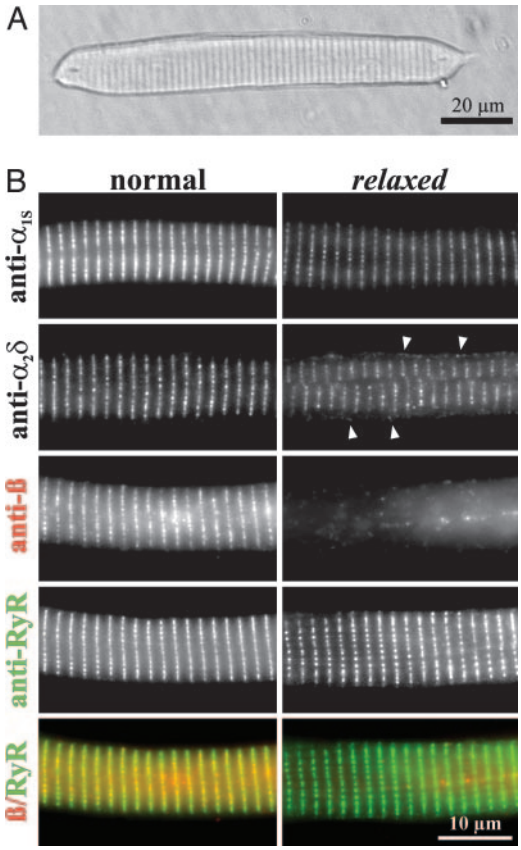

Fig. 3. Triad targeting properties of the DHPR subunits α_{1S}, $\alpha_2\delta$-1, and β_{1a} in myotubes from zebrafish mutant *relaxed* differ from those in normal myotubes. (*A*) Typical appearance of an adherent zebrafish myotube isolated from larval tail muscle and visualized by Hoffman modulation contrast (36). No morphological differences could be observed between *relaxed* and normal myotubes. (*B*) Immunofluorescence labeling of normal (*Left*) and *relaxed* (*Right*) myotubes with mAB 1A against α_{1S} (*Top*) showed correct triad clustering of the α_{1S} subunits in *relaxed*, although at a reduced level. Staining of *relaxed* myotubes with mAB 20A against $\alpha_2\delta$-1 (*Upper Middle*) showed that a fraction of the $\alpha_2\delta$-1 subunit is normally clustered in triads whereas another fraction is mistargeted diffusely into the plasma membrane (arrowheads), presumably because of the reduction in α_{1S} subunit levels (7, 33). In contrast to normal myotubes, immunostaining of *relaxed* myotubes with the pan-β antibody RCP6 (*Middle*) did not show any triadic staining, thus clearly demonstrating the β_{1a}-null phenotype of the *relaxed* zebrafish. Double immunofluorescence labeling of the same myotubes with mAB 34-C against RyR (*Lower Middle*) showed identical triadic clustered staining in normal and *relaxed*. The merged image (*Bottom*) emphasizes the colocalization (yellow foci) of RyR1 (green) and β_{1a} (red) in triadic clusters of normal myotubes.

the $\alpha_2\delta$-1 subunit is localized in the triads, whereas this subunit is also present in the plasma membrane in *relaxed* myotubes (Fig. 3*B*). The appearance of $\alpha_2\delta$-1 in the plasma membrane of *relaxed* myotubes suggests that, because of reduced α_{1S} expression in the absence of β_{1a}, $\alpha_2\delta$-1 is in excess of α_{1S}, and some of it remains diffusely distributed in the plasma membrane. Thus, regulation of membrane expression of α_{1S} and $\alpha_2\delta$-1 is independent from each other, and only membrane expression levels of α_{1S}, but not of $\alpha_2\delta$-1, depend on β_{1a}.

Electrophysiological recordings indicated a substantial reduction of the DHPR-specific maximum intramembrane charge movement (Q_{max}) (17) in *relaxed* myotubes (Fig. 4*C*). Q_{max} represents the maximum amount of α_{1S} gating charges moving across the membrane upon depolarization and is considered to be an accurate measure of functionally expressed α_{1S}. Q_{max} values in *relaxed* myotubes were reduced by ≈7.4-fold compared to normal.

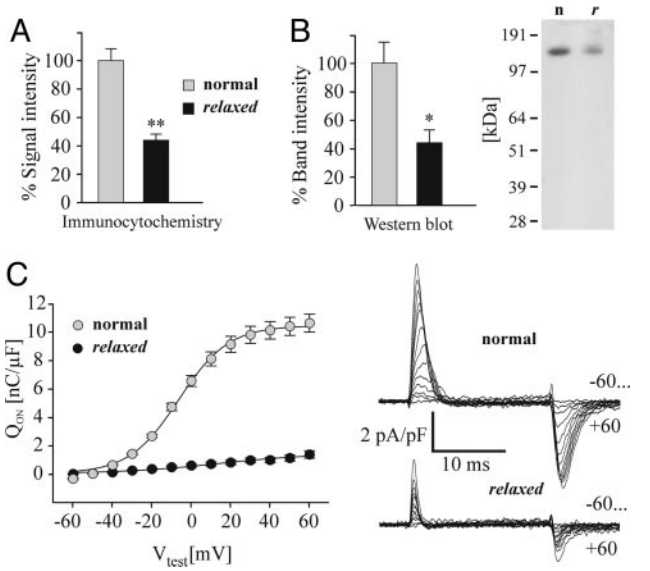

Fig. 4. The DHPR α_{1S} subunit is significantly reduced in *relaxed* compared with normal zebrafish skeletal muscle. (*A*) Quantification of the α_{1S} (antibody mAB 1A) immunofluorescence signal intensity in normal and *relaxed* myotubes (for details, see *Materials and Methods*) indicated a reduction of α_{1S} expression in *relaxed* myotubes to 44 ± 4% (**, $P < 0.001$; $n = 10$; paired *t* test). (*B*) mAB 1A staining intensity quantification (TINA 2.09c, Raytest Isotopenmessgeräte) after Western blot analysis indicated that the α_{1S} protein band intensity from *relaxed* tail muscle protein preparations was reduced to 45 ± 6% compared to normal (*, $P < 0.02$). A representative Western blot experiment out of five is shown at *Right*; n indicates normal, and *r* indicates *relaxed* zebrafish. (*C*) (*Left*) Average (±SE) intramembrane charge movements (Q_{on}) obtained from normal (gray circle, $n = 15$) or *relaxed* (black circle, $n = 12$) myotubes. Q_{on} was determined by integrating the "ON" outward current at each membrane potential and normalizing it to cell capacitance (nC/μF). Average (±SE) maximum intramembrane charge movement (Q_{max}) was 10.4 ± 0.6 ($n = 15$) for normal and 1.4 ± 0.2 ($n = 12$) nC/μF for *relaxed* myotubes ($P < 0.001$). (*Right*) Representative charge movement recordings from normal (*Upper*) and *relaxed* (*Lower*) myotubes in response to 20-ms depolarizations to membrane potentials between −60 and +60 mV applied in 10-mV increments.

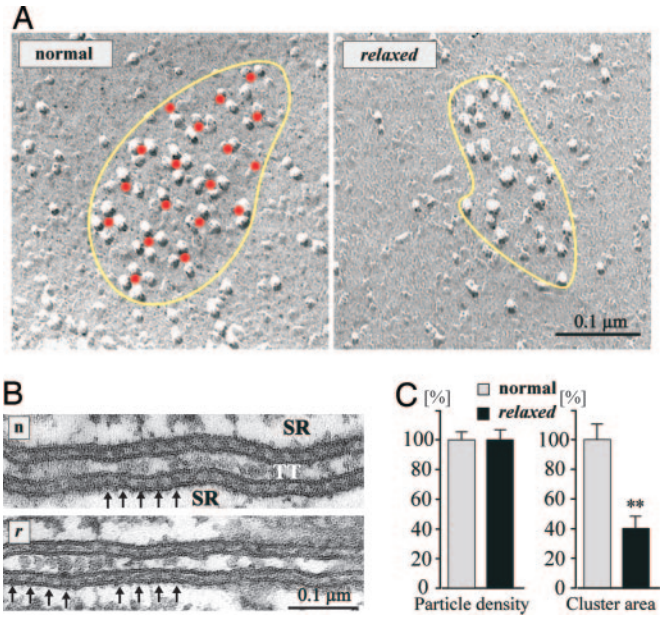

Fig. 5. Skeletal muscle of zebrafish β_{1a}-null mutant *relaxed* is lacking DHPR tetrad formation. (*A*) Freeze-fracture replicas of zebrafish tail myotubes showing the cytoplasmic leaflet of the plasmalemma. In myotubes from normal zebrafish (*Left*), small, slightly domed membrane areas (indicated in yellow) are occupied by large integral membrane particles, representing DHPRs. DHPRs are grouped into tetrads (groups of up to four), and the tetrads in turn are regularly arranged in an orthogonal array, as indicated by the red dots marking their centers. The membrane between the tetrads is clear of additional particles. *Relaxed* zebrafish muscle cells also show clusters of large particles in domed membrane areas (*Right*). However, these particles are not arranged in tetrads or orthogonal arrays. (*B*) Sections along the transverse tubules and triads from normal (n) and *relaxed* (*r*) myotubes in 3-day-old larvae. RyR1 (feet, indicated by arrows) maintain their orderly disposition. (*C*) Relative particle densities and cluster area from normal and *relaxed* myotubes. Particle density was 1,813 ± 69/324 particles per μm^2 (mean ± SE/SD; *n*, number of patches = 22) for normal and 1,814 ± 89/445 ($n = 25$) for *relaxed* myotubes. Average (± SE/SD) cluster area was 0.02 ± 0.002/0.009 μm^2 ($n = 22$) for normal and 0.008 ± 0.0005/0.003 μm^2 ($n = 25$) for *relaxed* myotubes. Whereas particle densities were indistinguishable, the reduction of cluster area to 40 ± 7% in *relaxed* is statistically significant (**, $P < 0.001$).

Apparently, there is a discrepancy between the ≈2.2-fold reduction in α_{1S} expression levels and the substantial reduction of Q_{max}. Because we cannot exclude the possibility that other ion channels, which are not blocked by our prepulse procedure (1 s to −30 mV; 70 ms to −50 mV; ref. 17), also contribute to the measured Q_{max}, the difference between DHPR-specific Q in normal and *relaxed* myotubes could be even more pronounced; this would indicate that without the β_{1a} subunit many of the DHPRs in the membrane are deficient in voltage-sensing. Such a defect could be induced by the loss of an allosteric action of β_{1a} on α_{1S} or by the disintegration of a putative cooperative effect of α_{1S} arranged in tetrads (see below). In contrast, if the possible contribution of Ca^{2+}-sensitive ion channels to Q_{max} is less than in normal myotubes because of missing Ca^{2+} transients in *relaxed* muscle, the discrepancy between the reduction in α_{1S} expression levels and DHPR-specific Q could be much smaller. In this case, most of the membrane expressed DHPRs in *relaxed* myotubes would still be functional voltage sensors.

The skeletal muscle-specific characteristic of the DHPR is its direct coupling with the RyR, evident in Ca^{2+}-independent EC coupling and the correlating structural organization of DHPRs in tetrad arrays in the junctional membranes of triads and peripheral couplings. Thus, an alternative explanation of the EC-coupling defect in *relaxed* zebrafish would be that the lack of β_{1a} somehow disengages the coupling of α_{1S} to the RyR1. Freeze-fracture analysis was performed on peripheral couplings because technical limitations do not allow obtaining images of the fractured transverse tubule membrane from the small larval myotubes. Similar results, as in isolated zebrafish myotubes, were obtained in 30-h-old whole embryo muscles (data not shown). The inner leaflet of the fractured plasmalemma of zebrafish myotubes revealed small domed membrane domains studded with groups of large intramembrane particles, which correspond to the DHPR clusters seen in immunofluorescence labeling (25, 34). In normal zebrafish myotubes, the DHPRs are arranged in tetrads that form regular orthogonal arrays (Fig. 5*A*). However, the corresponding domains of *relaxed* myotubes displayed a random distribution of particles, despite the normal organization of RyRs in arrays of "feet" as seen in sections of triads (Fig. 5*B*). The irregular distribution of DHPR particles seen in *relaxed* myotubes is therefore not due to a defect in the disposition of RyRs. This distribution is reminiscent of that detected in cardiac muscle and in α_{1S}-null myotubes expressing skeletal/cardiac α_1 subunit chimeras that are unable to support skeletal muscle EC coupling (25). The overall density of particles within these clusters was similar in normal and *relaxed* myotubes (Fig. 5*C*). However, in agreement with the reduced amount of α_{1S} immunofluorescence and protein (Fig. 4 *A* and *B*), the area of the DHPR clusters, and consequently the number of DHPRs/cluster in *relaxed* myotubes, was reduced to 40 ± 7% (Fig. 5*C*). Thus, the lack of the β_{1a} subunit in *relaxed* zebrafish partially reduces but

PHYSIOLOGY

does not eliminate membrane expression and triad targeting of the α_{1S} subunit, but significantly affects the physical coupling of the DHPR to the RyR1.

The observed reduction in the overall α_{1S} membrane concentration might indicate an independent and nonessential role of β_{1a} in DHPR membrane expression. However, it is also conceivable that DHPR complexes devoid of β_{1a} are less stable, possibly because of a conformational modification or because they are not anchored to RyR1, and are therefore subject to a higher turnover rate than fully assembled channels. Another possibility is that the lack of Ca^{2+} signals during development somehow diminishes α_{1S} expression, as observed in RyR1-null myotubes (35).

In summary, we distinguished three distinct effects of the β_{1a}-null mutant in skeletal muscle: An ≈50% reduction of DHPR membrane expression, which by itself is not sufficient to explain the loss of EC coupling; severely reduced gating charge movement, which could indicate a possible role of the β_{1a} subunit on the voltage-sensing function of the DHPR; and, most importantly, the complete loss of tetrad formation, which by itself can explain the failure of EC coupling in β_{1a}-null muscle cells. The present findings demonstrate that β_{1a} is absolutely required for tetrad formation and thus physical DHPR-RyR interaction. Whether it functions exclusively in physically coupling the α_{1S} with the RyR1 and thus enabling EC coupling or whether β_{1a} actively participates in the signal-transduction between the voltage-sensor and the Ca^{2+} release channel remains to be shown.

We thank Dr. H.-G. Frohnhöfer (Max Planck Institute, Tübingen, Germany) for the zebrafish mutant *relaxed*, Dr. J. Striessnig (University of Innsbruck, Innsbruck, Austria) for the pan-β antibody RCP6, and Dr. H. Glossmann for continuous support. This work was supported in part by the Austrian Science Fund and Austrian National Bank Grants P16098-B11 (to M.G.), P16532-B05 (to B.E.F.), and P17807-B05 (to G.J.O.); European Commission's IHP Grant HPRN-CT-2002-00331 (to B.E.F.); and National Institutes of Health Grant AR P01144650 (to C.F.-A.).

1. Armstrong, C. M., Bezanilla, F. M. & Horowicz, P. (1972) *Biochim. Biophys. Acta* **267,** 605–608.
2. Schneider, M. F. & Chandler, W. K. (1973) *Nature* **242,** 244–246.
3. Rios, E. & Brum, G. (1987) *Nature* **325,** 717–720.
4. Block, B. A., Imagawa, T., Campbell, K. P. & Franzini-Armstrong, C. (1988) *J. Cell Biol.* **107,** 2587–2600.
5. Arikkath, J. & Campbell, K. P. (2003) *Curr. Opin. Neurobiol.* **13,** 298–307.
6. Freise, D., Held, B., Wissenbach, U., Pfeifer, A., Trost, C., Himmerkus, N., Schweig, U., Freichel, M., Biel, M., Hofmann, F., *et al.* (2000) *J. Biol. Chem.* **275,** 14476–14481.
7. Obermair, G. J., Kugler, G., Baumgartner, S., Tuluc, P., Grabner, M. & Flucher, B. E. (2005) *J. Biol. Chem.* **280,** 2229–2237.
8. Gregg, R. G., Messing, A., Strube, C., Beurg, M., Moss, R., Behan, M., Sukhareva, M., Haynes, S., Powell, J. A., Coronado, R., *et al.* (1996) *Proc. Natl. Acad. Sci. USA* **93,** 13961–13966.
9. Tanabe, T., Beam, K. G., Powell, J. A. & Numa, S. (1988) *Nature* **336,** 134–139.
10. Strube, C., Beurg, M., Powers, P. A., Gregg, R. G. & Coronado, R. (1996) *Biophys. J.* **71,** 2531–2543.
11. Strube, C., Beurg, M., Sukhareva, M., Ahern, C. A., Powell, J. A., Powers, P. A., Gregg, R. G. & Coronado, R. (1998) *Biophys. J.* **75,** 207–217.
12. Beurg, M., Sukhareva, M., Ahern, C. A., Conklin, M. W., Perez-Reyes, E., Powers, P. A., Gregg, R. G. & Coronado, R. (1999) *Biophys. J.* **76,** 1744–1756.
13. Granato, M., van Eeden, F. J., Schach, U., Trowe, T., Brand, M., Furutani-Seiki, M., Haffter, P., Hammerschmidt, M., Heisenberg, C. P., Jiang, Y. J., *et al.* (1996) *Development (Cambridge, U.K.)* **123,** 399–413.
14. Ono, F., Higashijima, S., Shcherbatko, A., Fetcho, J. R. & Brehm, P. (2001) *J. Neurosci.* **21,** 5439–5448.
15. Flucher, B. E., Andrews, S. B. & Daniels, M. P. (1994) *Mol. Biol. Cell* **5,** 1105–1118.
16. Weiss, R. G., O'Connell, K. M., Flucher, B. E., Allen, P. D., Grabner, M. & Dirksen, R. T. (2004) *Am. J. Physiol.* **287,** C1094–C1102.
17. Adams, B. A., Tanabe, T., Mikami, A., Numa, S. & Beam, K. G. (1990) *Nature* **346,** 569–572.
18. Cheung, A., Dantzig, J. A., Hollingworth, S., Baylor, S. M., Goldman, Y. E., Mitchison, T. J. & Straight, A. F. (2002) *Nat. Cell. Biol.* **4,** 83–88.
19. Grabner, M., Friedrich, K., Knaus, H. G., Striessnig, J., Scheffauer, F., Staudinger, R., Koch, W. J., Schwartz, A. & Glossmann, H. (1991) *Proc. Natl. Acad. Sci. USA* **88,** 727–731.
20. Ruth, P., Rohrkasten, A., Biel, M., Bosse, E., Regulla, S., Meyer, H. E., Flockerzi, V. & Hofmann, F. (1989) *Science* **245,** 1115–1118.
21. Morton, M. E. & Froehner, S. C. (1987) *J. Biol. Chem.* **262,** 11904–11907.
22. Morton, M. E. & Froehner, S. C. (1989) *Neuron* **2,** 1499–1506.
23. Pichler, M., Cassidy, T. N., Reimer, D., Haase, H., Kraus, R., Ostler, D. & Striessnig, J. (1997) *J. Biol. Chem.* **272,** 13877–13882.
24. Glossmann, H. & Ferry, D. R. (1985) *Methods Enzymol.* **109,** 513–550.
25. Takekura, H., Paolini, C., Franzini-Armstrong, C., Kugler, G., Grabner, M. & Flucher, B. E. (2004) *Mol. Biol. Cell* **15,** 5408–5419.
26. Haffter, P., Granato, M., Brand, M., Mullins, M. C., Hammerschmidt, M., Kane, D. A., Odenthal, J., van Eeden, F. J., Jiang, Y. J., Heisenberg, C. P., *et al.* (1996) *Development (Cambridge, U.K.)* **123,** 1–36.
27. Mendel, J. G. (1866) *Verh. Nat. Vereins Brünn* **4**, 3–47.
28. Van Petegem, F., Clark, K. A., Chatelain, F. C. & Minor, D. L., Jr. (2004) *Nature* **429,** 671–675.
29. Opatowsky, Y., Chen, C. C., Campbell, K. P. & Hirsch, J. A. (2004) *Neuron* **42,** 387–399.
30. Sheridan, D. C., Cheng, W., Ahern, C. A., Mortenson, L., Alsammarae, D., Vallejo, P. & Coronado, R. (2003) *Biophys. J.* **84,** 220–237.
31. Dolphin, A. C. (2003) *J. Bioenerg. Biomembr.* **35,** 599–620.
32. Bichet, D., Cornet, V., Geib, S., Carlier, E., Volsen, S., Hoshi, T., Mori, Y. & De Waard, M. (2000) *Neuron* **25,** 177–190.
33. Flucher, B. E., Phillips, J. L. & Powell, J. A. (1991) *J. Cell Biol.* **115,** 1345–1356.
34. Protasi, F., Franzini-Armstrong, C. & Allen, P. D. (1998) *J. Cell Biol.* **140,** 831–842.
35. Avila, G., O'Connell, K. M., Groom, L. A. & Dirksen, R. T. (2001) *J. Biol. Chem.* **276,** 17732–17738.
36. Hoffman, R. & Gross, L. (1975) *Nature* **254,** 586–588.